Electronic Supplementary Material (ESI) for Materials Advances.

Supporting Information

Tuning the switching pressure in square lattice coordination networks by metal cation substitution

*Shi-Qiang Wang, Shaza Darwish, Debobroto Sensharma, Michael J. Zaworotko**

Bernal Institute and Department of Chemical Sciences, University of Limerick, Limerick V94 T9PX, Republic of Ireland.

**E-mail:* Michael.Zaworotko@ul.ie

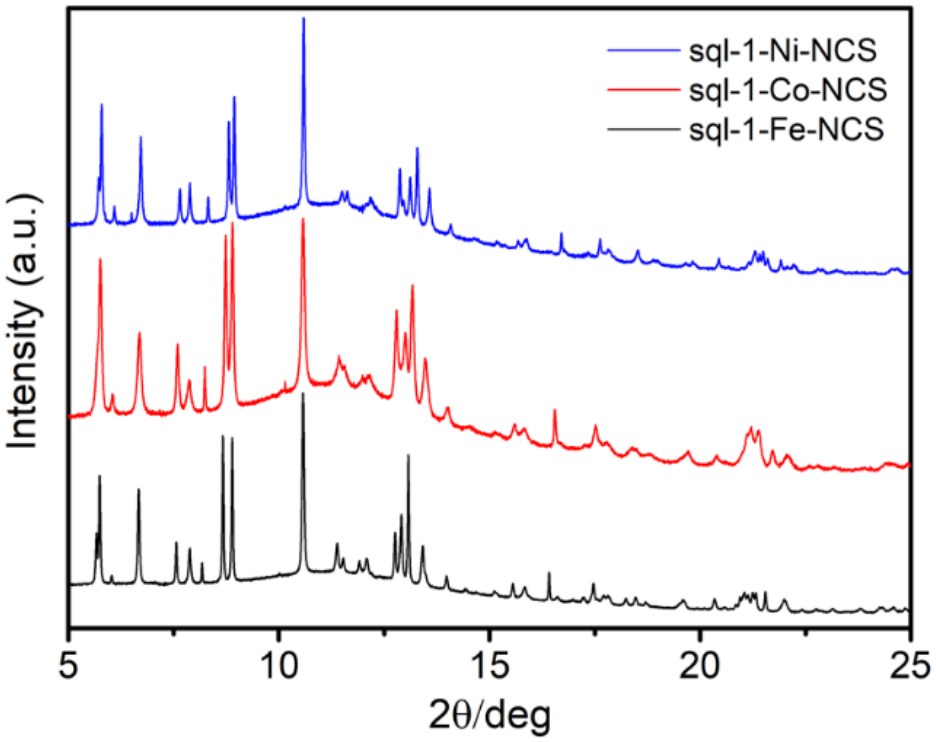

Figure S1. Synchrotron PXRD patterns of **sql-1-M-NCS** (M = Fe, Co and Ni).

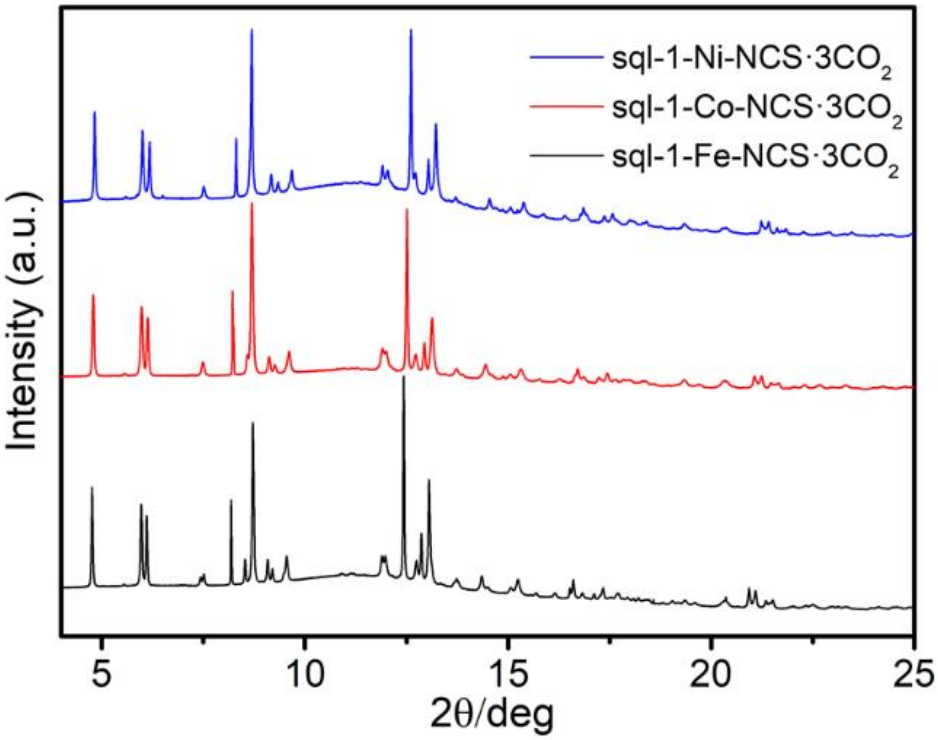

Figure S2. Synchrotron PXRD patterns of **sql-1-M-NCS·3CO$_2$** (M = Fe, Co and Ni).

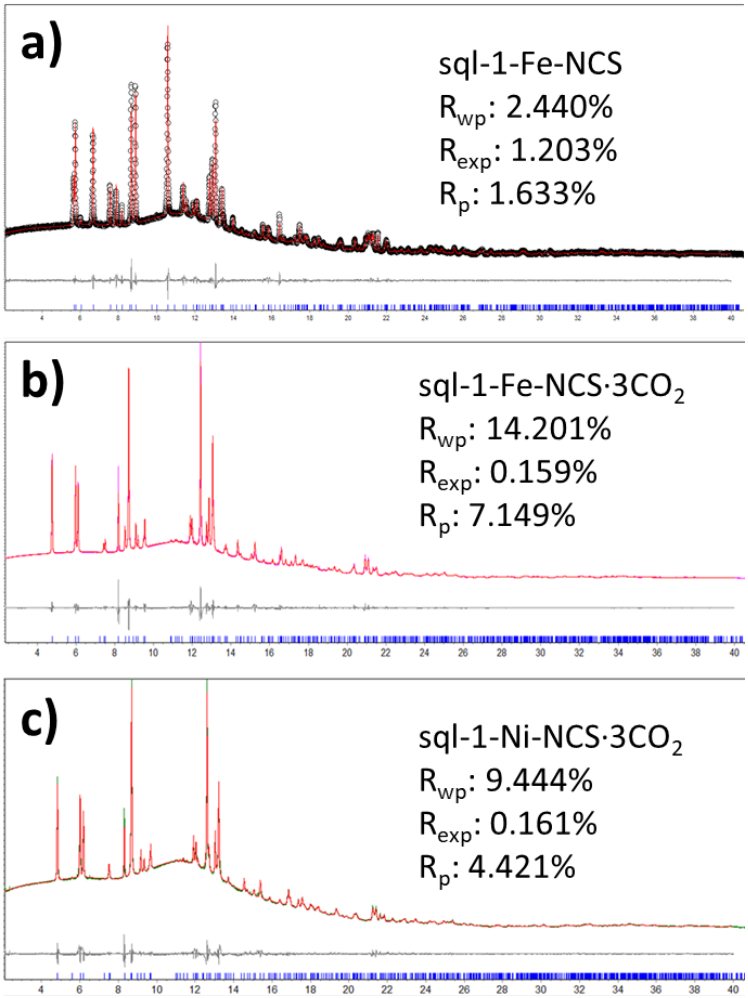

Figure S3. Rietveld refinement results for a) **sql-1-Fe-NCS**, b) **sql-1-Fe-NCS·3CO_2** and c) **sql-1-Ni-NCS·3CO_2.**

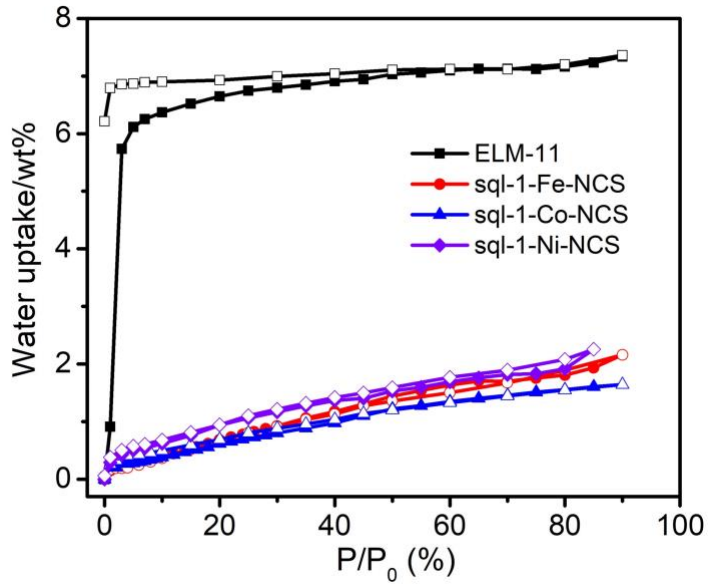

Figure S4. Water vapour sorption for ELM-11 and **sql-1-M-NCS** at 298 K.

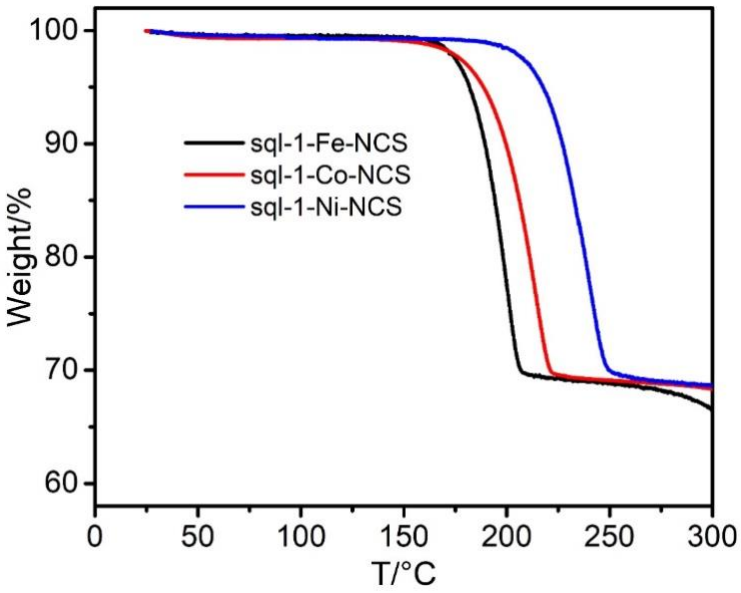

Figure S5. TGA curves of **sql-1-M-NCS** (M = Fe, Co and Ni).

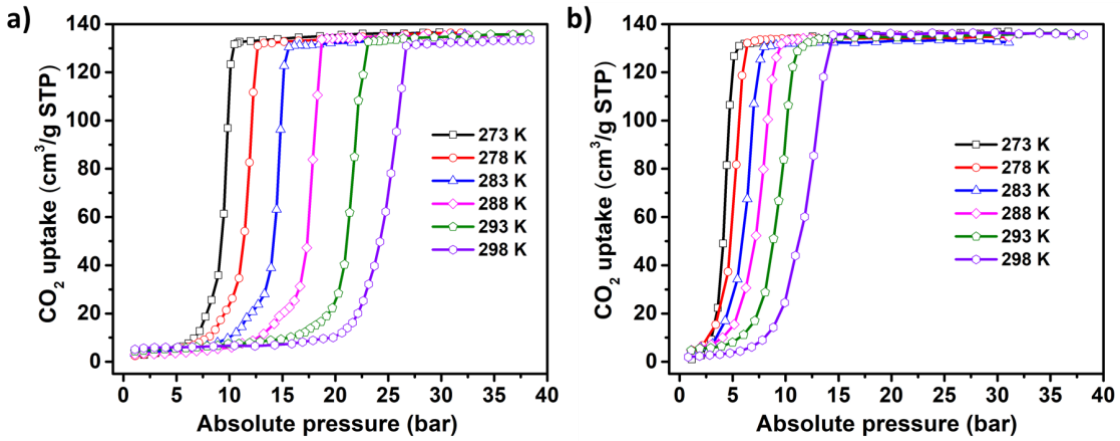

Figure S6. High-pressure CO_2 desorption isotherms of a) **sql-1-Fe-NCS** and b) **sql-1-Ni-NCS**.

T/K	sql-1-Fe-NCS		sql-1-Ni-NCS	
	P_{ga}/bar	P_{gd}/bar	P_{ga}/bar	P_{gd}/bar
273	12.5	10.5	6.5	5.1
278	15.2	12.8	8.1	6.4
283	18.5	15.5	10.1	7.9
288	22.3	18.7	12.5	9.8
293	26.6	22.6	15.2	11.9
298	31.6	26.7	18.5	14.5

sql-1-Fe-NCS	sql-1-Ni-NCS
$\ln P_{ga} = -3024/T + 13.60$	$\ln P_{ga} = -3410/T + 14.36$
$\ln P_{gd} = -3050/T + 13.52$	$\ln P_{gd} = -3395/T + 14.07$

Equation	y = a + b*x	sql-1-Fe-NCS	
Weight	No Weighting		P_{ga}
Intercept	13.60304 ± 0.02996		
Slope	-3.02429 ± 0.0854		
Residual Sum of Squares		1.92895E-5	
Pearson's r		-0.99998	
R-Square(COD)		0.99997	
Adj. R-Square		0.99996	

Equation	y = a + b*x	sql-1-Ni-NCS	
Weight	No Weighting		P_{ga}
Intercept	14.36001 ± 0.0422		
Slope	-3.40958 ± 0.01203		
Residual Sum of Squares		3.82764E-5	
Pearson's r		-0.99998	
R-Square(COD)		0.99995	
Adj. R-Square		0.99994	

Equation	y = a + b*x	sql-1-Fe-NCS	
Weight	No Weighting		P_{gd}
Intercept	13.5226 ± 0.05396		
Slope	-3.05035 ± 0.01539		
Residual Sum of Squares		6.25838E-5	
Pearson's r		-0.99995	
R-Square(COD)		0.9999	
Adj. R-Square		0.99987	

Equation	y = a + b*x	sql-1-Ni-NCS	
Weight	No Weighting		P_{gd}
Intercept	14.06747 ± 0.04373		
Slope	-3.39533 ± 0.01247		
Residual Sum of Squares		4.10981E-5	
Pearson's r		-0.99997	
R-Square(COD)		0.99995	
Adj. R-Square		0.99993	

Figure S7. The linear fit parameters and results yielded from Clausius-Clapeyron equation.

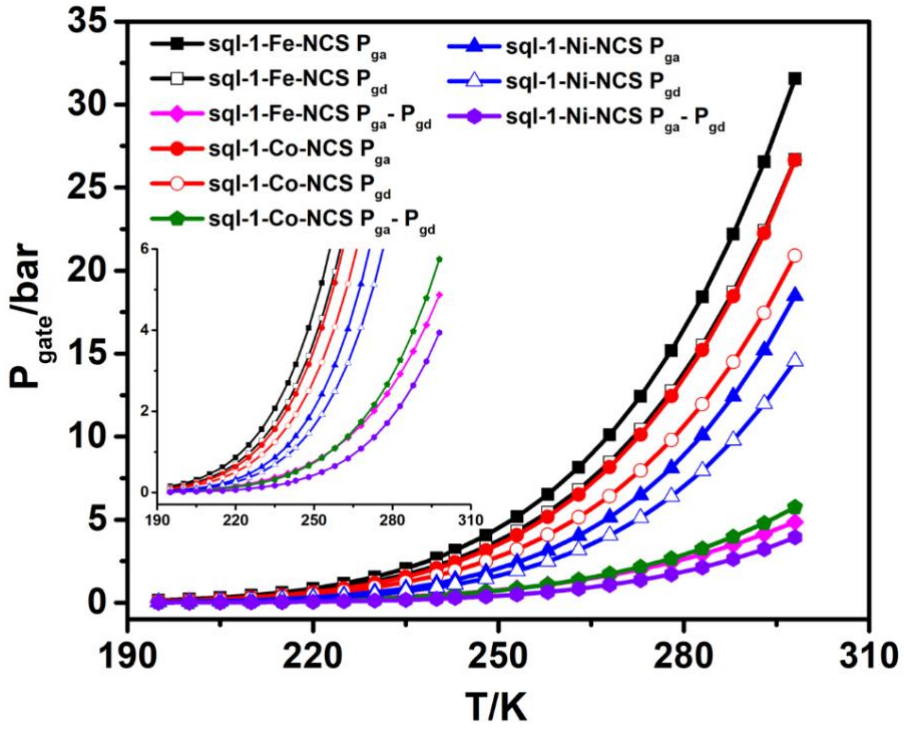

Figure S8. Calculated P_{ga}/P_{gd} and hysteresis gaps for **sql-1-M-NCS** (M = Fe, Co and Ni).

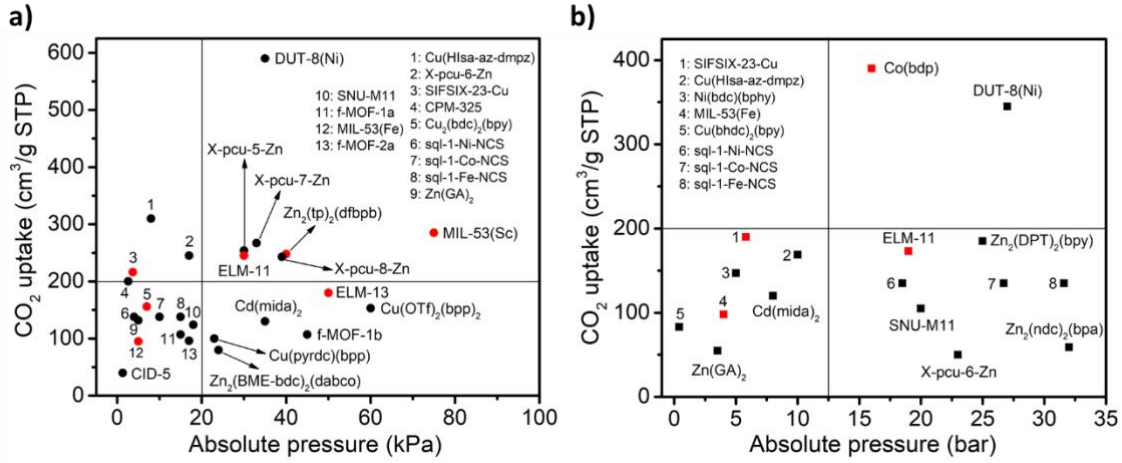

Figure S9. Comparison of switching CNs with respect to CO_2 switching pressures and uptakes at a) 195 and b) 298 K. Black and red symbols denote CNs with type F-IV^s and F-IV^m isotherms respectively. For type F-IV^m isotherms, only the switching pressures of the last step are shown (see table S2 for details).

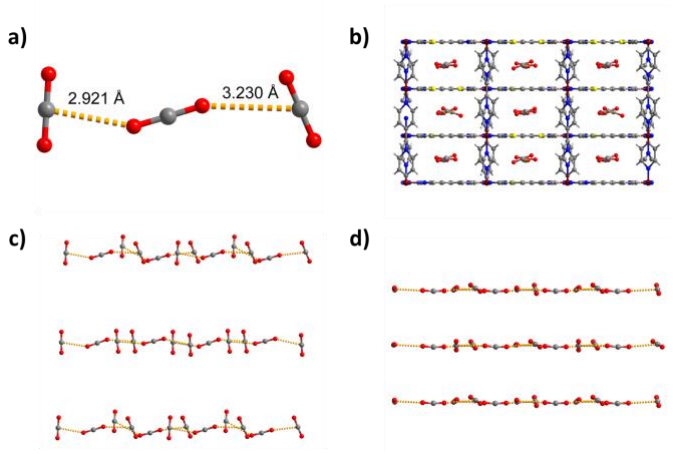

Figure S10. a) one $[CO_2]_3$ cluster unit in **sql-1-Fe-NCS·3CO₂** and b-d) CO_2 packing modes along a, b, c axis, respectively. Network structures along b and c axes are omitted for clarity.

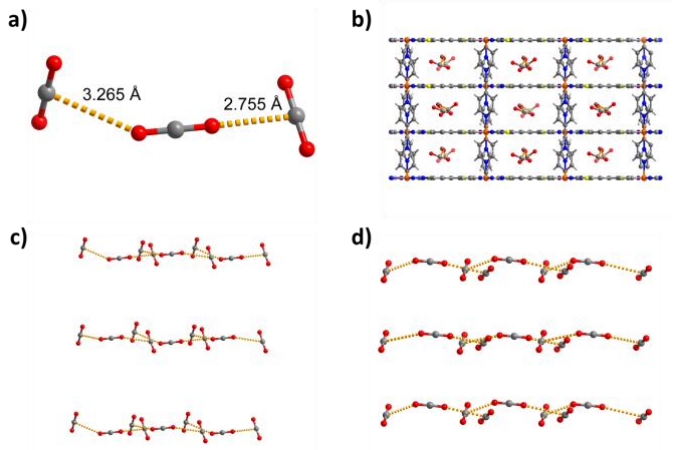

Figure S11. a) one $[CO_2]_3$ cluster unit in **sql-1-Co-NCS·3CO₂** and b-d) the packing modes along a, b, c axis, respectively. Network structures along b and c axes are omitted for clarity.

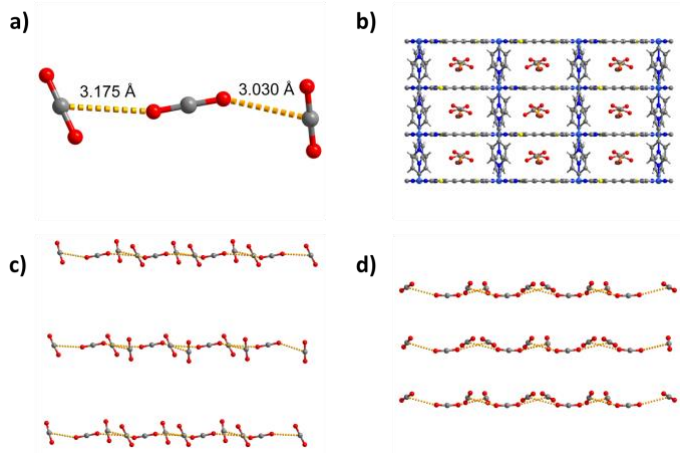

Figure S12. a) one $[CO_2]_3$ cluster unit in **sql-1-Ni-NCS·3CO₂** and b-d) the packing modes along a, b, c axis, respectively. Network structures along b and c axes are omitted for clarity.

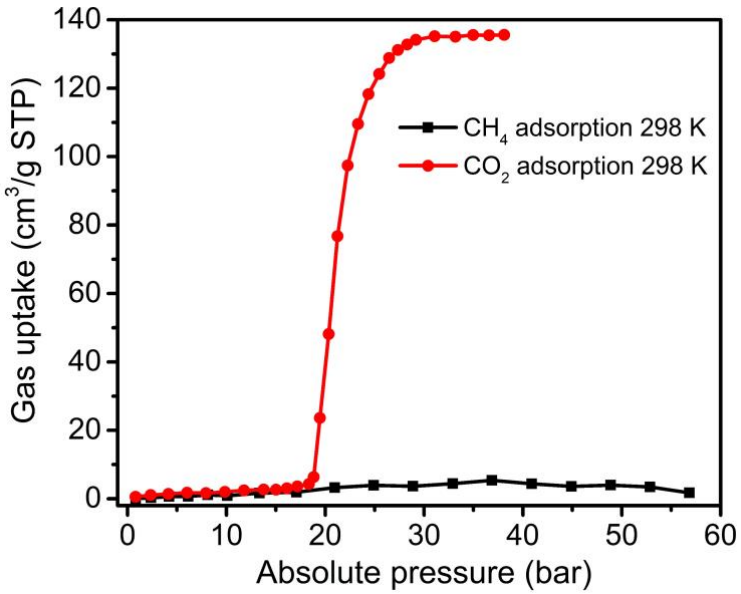

Figure S13. High-pressure CH_4 vs. CO_2 adsorption isotherms of **sql-1-Ni-NCS.**

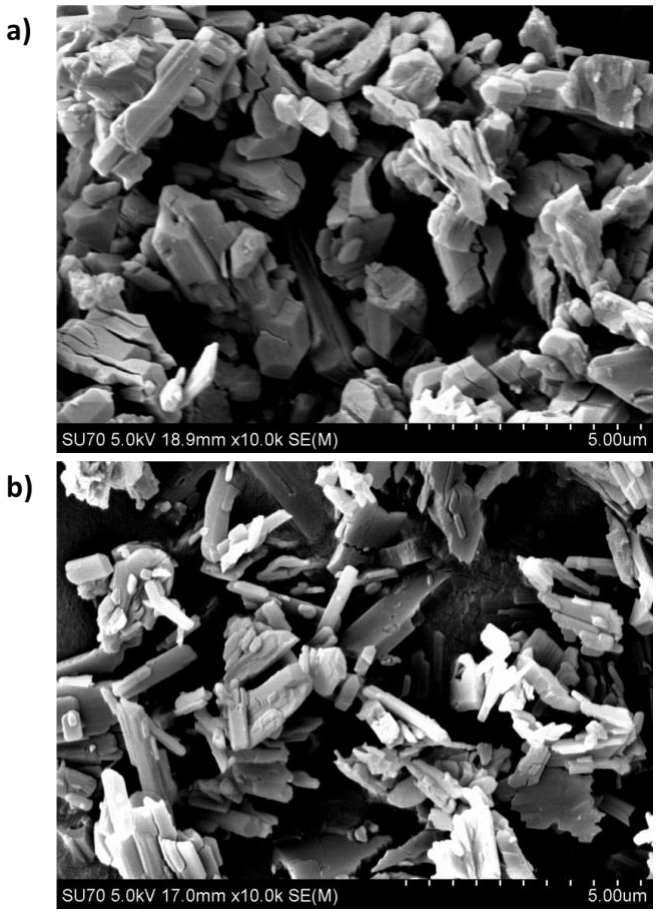

Figure S14. SEM images of a) **sql-1-Fe-NCS** and b) **sql-1-Ni-NCS.**

Table S1. Calculated CO_2 switching pressures (P_{ga}/P_{gd}) and hysteresis gaps (P_{ga} - P_{gd}) for **sql-1-M-NCS** (M= Fe, Co and Ni).

T/K	sql-1-Fe-NCS			sql-1-Co-NCS			sql-1-Ni-NCS		
	P_{ga}/bar	P_{gd}/bar	(P_{ga} – P_{gd})/bar	P_{ga}/bar	P_{gd}/bar	(P_{ga} – P_{gd})/bar	P_{ga}/bar	P_{gd}/bar	(P_{ga} – P_{gd})/bar
195	0.15	0.12	0.03	0.1	0.08	0.02	0.04	0.035	0.005
200	0.22	0.18	0.04	0.15	0.12	0.03	0.07	0.055	0.015
205	0.32	0.26	0.06	0.22	0.18	0.04	0.1	0.08	0.02
210	0.45	0.37	0.08	0.32	0.25	0.07	0.15	0.12	0.03
215	0.63	0.51	0.12	0.45	0.36	0.09	0.22	0.18	0.04
220	0.86	0.71	0.15	0.63	0.5	0.13	0.32	0.26	0.06
225	1.17	0.96	0.21	0.86	0.68	0.18	0.45	0.36	0.09
230	1.57	1.29	0.28	1.17	0.93	0.24	0.63	0.5	0.13
235	2.08	1.72	0.36	1.56	1.24	0.32	0.86	0.69	0.17
240	2.72	2.25	0.47	2.07	1.64	0.43	1.16	0.93	0.23
243	3.18	2.63	0.55	2.43	1.92	0.51	1.39	1.1	0.29
248	4.08	3.39	0.69	3.16	2.5	0.66	1.84	1.46	0.38
253	5.19	4.33	0.86	4.06	3.21	0.85	2.42	1.92	0.5
258	6.55	5.46	1.09	5.17	4.08	1.09	3.14	2.49	0.65
263	8.18	6.84	1.34	6.52	5.14	1.38	4.03	3.19	0.84
268	10.1	8.49	1.62	8.16	6.42	1.74	5.14	4.06	1.08
273	12.5	10.5	2.00	10.1	7.96	2.16	6.48	5.12	1.36
278	15.2	12.8	2.40	12.5	9.79	2.66	8.12	6.41	1.71
283	18.4	15.5	2.90	15.2	12	3.26	10.1	7.95	2.13
288	22.2	18.7	3.50	18.5	14.5	3.97	12.4	9.79	2.64
293	26.6	22.4	4.20	22.3	17.5	4.79	15.2	12	3.23
298	31.6	26.7	4.90	26.7	20.9	5.75	18.5	14.6	3.94

Table S2. Summary of CO_2 switching pressure and uptake for switching CNs.

Switching CNs	Dimension	P_{ga}/kPa	Uptake (cm^3g^{-1})	P_{ga}/bar	Uptake (cm^3g^{-1})	Isotherm type	ref.
		195 K		298 K			
DUT-8(Ni)	3D	35	590	27	345	F-IV^s	1
Co(bpd)	3D	N.A.	N.A.	2 ($P_{ga}1$)/ 5 ($P_{ga}2$)/ 16 ($P_{ga}3$)	90/ 220/ 390	F-IV^m	2
Cu(HIsa-az-dmpz)	3D	8	310	10	169	F-IV^s	3
MIL-53(Sc)	3D	5 ($P_{ga}1$)/ 75 ($P_{ga}2$)	65/ 285	N.A.	N.A.	F-IV^m	4
X-pcu-6-Zn	3D	17	245	23	50	F-IV^s	5,6
X-pcu-5-Zn	3D	30	254	remain closed up to 33 bar		F-IV^s	
X-pcu-7-Zn	3D	33	267			F-IV^s	
X-pcu-8-Zn	3D	39	243			F-IV^s	
$[Zn_2(tp)_2(dfbpb)]$	3D	5 ($P_{ga}1$)/ 40 ($P_{ga}2$)	90/ 248	N.A.	N.A.	F-IV^m	7
ELM-11	2D	0.3 ($P_{ga}1$)/ 30 ($P_{ga}2$)	82/ 245	0.65 ($P_{ga}1$)/ 19 ($P_{ga}2$)	80/ 173	F-IV^m	8
SIFSIX-23-Cu	3D	0.3 ($P_{ga}1$)/ 3.7 ($P_{ga}2$)	84/ 216	2 ($P_{ga}1$)/ 5.8 ($P_{ga}2$)	85/ 190	F-IV^m	9
CPM-325	3D	2.6	200	N.A.	N.A.	F-IV^s	10
$[Zn_2(DPT)_2(bpy)]$	3D	N.A.	N.A.	25	185	F-IV^s	11
ELM-13	2D	4 ($P_{ga}1$)/ 10 ($P_{ga}1$)/ 50 ($P_{ga}1$)	90/ 150/ 180	N.A.	N.A.	F-IV^m	12
$[Cu_2(bdc)_2(bpy)]$	3D	0.7 ($P_{ga}1$)/ 7 ($P_{ga}2$)	110/ 156	N.A.	N.A.	F-IV^m	13
$[Cu(OTf)_2(bpp)_2]$	1D	60	153	N.A.	N.A.	F-IV^s	14
[Ni(bdc)(bphy)]	2D	N.A.	131	5	147	F-IV^s	15
sql-1-Co-NCS	2D	10	138	26.7	135	F-IV^s	16
sql-1-Ni-NCS	2D	4	138	18.5	135	F-IV^s	Current work
sql-1-Fe-NCS	2D	15	138	31.6	135	F-IV^s	

$Zn(GA)_2$	3D	5	132	3.5	55	F-IV^s	17
$Cd(mida)_2$	3D	35	130	8	120	F-IV^s	18
SNU-M11	3D	18	124	20	105	F-IV^s	19
f-MOF-1a	3D	15	107	N.A.	N.A.	F-IV^s	20
f-MOF-1b	3D	40	107	N.A.	N.A.	F-IV^s	
f-MOF-2a	3D	17	96	N.A.	N.A.	F-IV^s	
[Cu(pyrdc)(bpp)]	2D	23	100	N.A.	N.A.	F-IV^s	21
MIL-53(Fe)	3D	5	95	0.08 ($P_{ga}1$)/ 4 ($P_{ga}2$)	30/ 98 (303 K)	F-IV^m	22
$[Cu(dhbc)_2(bpy)]$	2D	N.A.	N.A.	0.4	83	F-IV^s	23
$[Zn_2$(BME-bdc)$_2$(dabco)]	3D	24	80	N.A.	N.A.	F-IV^s	24
$[Zn_2(ndc)_2(bpa)]$	3D	N.A.	N.A.	32	59	F-IV^s	25
CID-5	2D	1.3	40	N.A.	N.A.	F-IV^s	26

Table S3. Crystallographic data of **sql-1-M-NCS** and their CO_2 loaded phases.

	sql-1-Fe-NCS	[a]**sql-1-Co-NCS**	**sql-1-Ni-NCS**
Formula	$Fe(C_{10}H_8N_2)_2(NCS)_2$	$Co(C_{10}H_8N_2)_2(NCS)_2$	$Ni(C_{10}H_8N_2)_2(NCS)_2$
Formula weight	484.38	487.46	487.24
Temperature/K	195	100	296
Crystal system	Monoclinic	Monoclinic	Monoclinic
Space group	*C2/c*	*C2/c*	*C2/c*
a/Å	12.169	12.099	12.156
b/Å	11.542	11.399	11.381
c/Å	16.671	16.538	16.646
β/°	100.33	99.94	100.43
Volume/Å^3	2303.7	2246.6	2264.9
Z	4	4	4
ρ_{calc} g/cm^3	1.40	1.44	1.43
ρ_{net} g/cm^3	1.40	1.44	1.43
	sql-1-Fe-NCS·3CO$_2$	[a]**sql-1-Co-NCS·3CO$_2$**	**sql-1-Ni-NCS·3CO$_2$**
Formula	$Fe(C_{10}H_8N_2)_2(NCS)_2{\cdot}3CO_2$	$Co(C_{10}H_8N_2)_2(NCS)_2{\cdot}3CO_2$	$Ni(C_{10}H_8N_2)_2(NCS)_2{\cdot}3CO_2$
Formula weight	616.42	619.50	619.26
Temperature/K	195	195	195
Crystal system	Monoclinic	Monoclinic	Monoclinic
Space group	*C2/c*	*C2/c*	*C2/c*
a/Å	12.582	12.605	12.601
b/Å	11.535	11.468	11.368
c/Å	19.806	19.684	19.563
β/°	92.57	92.92	93.41
Volume/Å^3	2871.6	2841.7	2797.3
Z	4	4	4
ρ_{calc} g/cm^3	1.43	1.45	1.47
ρ_{net} g/cm^3	1.12	1.14	1.16

a: Crystallographic data obtained from ref 16.

References

1. N. Klein, H. C. Hoffmann, A. Cadiau, J. Getzschmann, M. R. Lohe, S. Paasch, T. Heydenreich, K. Adil, I. Senkovska, E. Brunner and K, Stefan, *J. Mater. Chem.*, 2012, **22**, 10303-10312.
2. M. K. Taylor, T. Runčevski, J. Oktawiec, J. E. Bachman, R. L. Siegelman, H. Jiang, J. A. Mason, J. D. Tarver and J. R. Long, *J. Am. Chem. Soc.*, 2018, **140**, 10324-10331.
3. S. Millan, B. Gil-Hernandez, E. Milles, S. Gokpinar, G. Makhloufi, A. Schmitz, C. Schlusener and C. Janiak, *Dalton Trans*, 2019, **48**, 8057-8067.
4. J. P. Mowat, V. R. Seymour, J. M. Griffin, S. P. Thompson, A. M. Slawin, D. Fairen-Jimenez, T. Düren, S. E. Ashbrook and P. A. Wright, *Dalton Trans.*, 2012, **41**, 3937-3941.
5. A.-X. Zhu, Q.-Y. Yang, A. Kumar, C. Crowley, S. Mukherjee, K.-J. Chen, S.-Q. Wang, D. O'Nolan, M. Shivanna and M. J. Zaworotko, *J. Am. Chem. Soc.*, 2018, **140**, 15572-15576.
6. A.-X. Zhu, Q.-Y. Yang, S. Mukherjee, A. Kumar, C.-H. Deng, A. A. Bezrukov, M. Shivanna and M. J. Zaworotko, *Angew. Chem. Int. Ed.*, 2019, **58**, 18212-18217.
7. J. Seo, C. Bonneau, R. Matsuda, M. Takata and S. Kitagawa, *J. Am. Chem. Soc.*, 2011, **133**, 9005-9013.
8. M. Ichikawa, A. Kondo, H. Noguchi, N. Kojima, T. Ohba, H. Kajiro, Y. Hattori and H. Kanoh, *Langmuir*, 2016, **32**, 9722-9726.
9. B.-Q. Song, Q.-Y. Yang, S.-Q. Wang, M. Vandichel, A. Kumar, C. Crowley, N. Kumar, C.-H. Deng, V. GasconPerez, M. Lusi, H. Wu, W. Zhou and M. J. Zaworotko, *J. Am. Chem. Soc.*, 2020, **142**, 6896-6901.
10. J. Jin, X. Zhao, P. Feng and X. Bu, *Angew. Chem., Int. Ed.*, 2018, **57**, 3737-3741.
11. E. R. Engel, A. Jouaiti, C. X. Bezuidenhout, M. W. Hosseini and L. J. Barbour, *Angew. Chem. Int. Ed.*, 2017, **56**, 8874-8878.
12. A. Kondo, H. Kajiro, T. Nakagawa, H. Tanaka and H. Kanoh, *Dalton Trans.*, 2020, **49**, 3692-3699.
13. Y. Sakata, S. Furukawa, M. Kondo, K. Hirai, N. Horike, Y. Takashima, H. Uehara, N. Louvain, M. Meilikhov, T. Tsuruoka, S. Isoda, W. Kosaka, O. Sakata and S. Kitagawa, *Science*, 2013, **339**, 193-196.
14. K. Fukuhara, S.-i. Noro, K. Sugimoto, T. Akutagawa, K. Kubo and T. Nakamura, *Inorg. Chem.*, 2013, **52**, 4229-4237.
15. X.-M. Liu, R.-B. Lin, J.-P. Zhang and X.-M. Chen, *Inorg. Chem.*, 2012, **51**, 5686-5692.
16. S.-Q. Wang, Q.-Y. Yang, S. Mukherjee, D. O'Nolan, E. Patyk-Kaźmierczak, K.-J. Chen, M. Shivanna, C. Murray, C. C. Tang and M. J. Zaworotko, *Chem. Commun.*, 2018, **54**, 7042-7045.
17. J. Rabone, Y. F. Yue, S. Y. Chong, K. C. Stylianou, J. Bacsa, D. Bradshaw, G. R. Darling, N. G. Berry, Y. Z. Khimyak, A. Y. Ganin, P. Wiper, J. B. Claridge and M. J. Rosseinsky, *Science*, 2010, **329**, 1053-1057.
18. H. Yang, F. Guo, P. Lama, W.-Y. Gao, H. Wu, L. J. Barbour, W. Zhou, J. Zhang, B. Aguila and S. Ma, *ACS Cent. Sci.*, 2018, **4**, 1194-1200.

19. H. S. Choi and M. P. Suh, *Angew. Chem. Int. Ed.*, 2009, **48**, 6865-6869.

20. P. Kanoo, R. Haldar, S. K. Reddy, A. Hazra, S. Bonakala, R. Matsuda, S. Kitagawa, S. Balasubramanian and T. K. Maji, *Chem.- Eur. J.*, 2016, **22**, 15864-15873.

21. T. K. Maji, G. Mostafa, R. Matsuda and S. Kitagawa, *J. Am. Chem. Soc.*, 2005, **127**, 17152-17153.

22. N. Guillou, S. Bourrelly, P. L. Llewellyn, R. I. Walton and F. Millange, *CrystEngComm*, 2015, **17**, 422-429.

23. R. Kitaura, K. Seki, G. Akiyama and S. Kitagawa, *Angew. Chem. Int. Ed.*, 2003, **42**, 428-431.

24. A. Schneemann, P. Vervoorts, I. Hante, M. Tu, S. Wannapaiboon, C. Sternemann, M. Paulus, D. F. Wieland, S. Henke and R. A. Fischer, *Chem. Mater.*, 2018, **30**, 1667-1676.

25. A. Hazra, D. P. van Heerden, S. Sanyal, P. Lama, C. Esterhuysen and L. J. Barbour, *Chem. Sci.*, 2019, **10**, 10018-10024.

26. T. Fukushima, S. Horike, Y. Inubushi, K. Nakagawa, Y. Kubota, M. Takata and S. Kitagawa, *Angew. Chem. Int. Ed.*, 2010, **49**, 4820-4824.